



Characteristics and pore evolution of the tight sandstone reservoirs of the Chang-7 Member of the Yanchang Formation in the Xin'anbian area, Ordos basin

Jiale Xu^{1,2,3} · Jingdong Liu^{1,2,3} · Songtao Wu⁴ · Tao Liu^{1,2,3}

Accepted: 10 August 2020 / Published online: 26 August 2020
© Springer-Verlag GmbH Germany, part of Springer Nature 2020

Abstract

More than 100 million tons of tight oil reserves have been discovered in the Xin'anbian area of the Ordos basin in recent years, of which the main reservoir is the Chang-7 Member of the Yanchang Formation. To identify the characteristics of the tight sandstone reservoir and their the development of the Chang-7 Member in the study area, casting thin sections, scanning electron microscopy (SEM), high-pressure mercury injection, cathodoluminescence and other technical methods were used to analyze the reservoir rock types and their physical properties and pore structure. Based on reservoir diagenesis research and quantitative evaluations of reservoir pores, a reservoir pore evolution mode was established. The results showed that the main rock types in the tight sandstone reservoirs in the Chang-7 Member of the Xin'anbian area were lithic feldspathic sandstone and feldspathic detritus sandstone and that the reservoir space types were mainly feldspar dissolved pores, with a few residual intergranular pores, clay intercrystalline pores, and microfractures. The reservoirs were classified as having low porosity and low permeability and extra-low porosity and extra-low permeability. The porosity and permeability of the reservoirs were between 4~10% and 0.01~1 mD, respectively, and were mainly controlled by compaction, cementation, and dissolution. Compaction and cementation reduced the porosity and permeability, while dissolution increased the porosity and permeability. The Chang-7 Member reservoir mainly experienced weak-medium compaction, medium-strong cementation, and different degrees of dissolution. The average loss of porosity due to cementation was around 25%, while the average loss due to compaction was around 13%. This research determined four key stages in the porosity evolution of the Chang-7 Member in the study area: (1) the porosity was reduced to 26% from the Triassic to the Early Jurassic period, which was mainly due to compression compaction; (2) the reservoir was seriously damaged by cementation from the Middle Jurassic to Late Jurassic period, where the porosity decreased to 5%; (3) in the Early Cretaceous period, the porosity increased to 11% due to dissolution; and (4) the porosity was reduced to 7% from the late Early Cretaceous to early Late Cretaceous period, which was mainly due to cementation.

Keywords Ordos basin · Tight sandstone · Reservoir characteristics · Diagenesis · Pore evolution

Electronic supplementary material The online version of this article (<https://doi.org/10.1007/s13146-020-00625-1>) contains supplementary material, which is available to authorized users.

✉ Jingdong Liu
ljd840911@126.com
Jiale Xu
1637364084@qq.com

³ School of Geosciences, China University of Petroleum (East China), Qingdao 266580, China

⁴ Research Institute of Petroleum Exploration and Development, PetroChina, Beijing 100083, China

¹ Key Laboratory of Deep Oil and Gas, China University of Petroleum (East China), Qingdao 266580, China

² Shandong Provincial Key Laboratory of Reservoir Geology, China University of Petroleum (East China), Qingdao 266580, China

Introduction

Tight oil refers to the accumulation of oil in a reservoir that is economically productive only by means of large-scale fracturing. The porosity of tight reservoirs is generally less than 10%, while the permeability is generally less than 1 mD (Zhao et al. 2012; Wu et al. 2018). Tight oil is one of the most important unconventional oil and gas resources in the world and is important for increasing the production of oil fields, which are characterized by wide area distribution, low oil quality density, short migration distance, and great resource potential (Sun et al. 2011; Liang et al. 2011). As one of the most important tight reservoirs, tight sandstone reservoirs are characterized by lithologic compactness, low porosity, and low permeability (Zou et al. 2010, 2013a, b). China has wide tight oil distribution, and at present, tight oil exploration shows good development prospects. It has become a hot spot for people to find relatively good quality reservoirs on the basis of tight sandstone reservoirs with low porosity and low permeability (Wang et al. 2014; Fan 2016).

The Ordos basin has the richest tight oil resources in China, accounting for about one quarter of the country's total tight oil resources (Meng et al. 2018). The Yanchang Formation of the Triassic system in the Ordos basin has huge tight oil reserves (Yao et al. 2013), of which the Chang-7 Member is the main area of tight oil exploration. One hundred million tons of proven tight oil reserves were found in the Chang-7 Member reservoir of the Xin'anbian area in 2014 (Wu et al. 2018). The pore throat structure of tight oil reservoirs is more complex and heterogeneous than conventional reservoirs. According to research on the micro-pore structure of tight oil reservoirs in the Chang 7 Member of the Ordos basin by Zou et al. (2012), nanoporous pores are the main reservoir space for tight oil. You et al. (2014) state that micron pores larger than two microns constitute the main reservoir space in tight oil reservoirs. Zhang et al. (2017) state that the pore radius of the Chang-7 Member reservoir in the Xin'anbian area is largely between 0 and 0.5 microns, and the throat radius is largely between 15 and 380 nm. In terms of reservoir densification in the study area, Wang (2018) argues that compaction is the main cause of reservoir densification, while Chu et al. (2013) state that the diagenesis intensity differs for different diagenetic facies and that the densification of Yanchang Formation is mainly controlled by compaction and cementation. However, previous studies have focused on reservoir characteristics but lack in-depth analysis on the differences in reservoir diagenesis intensity and reservoir densification (Yao et al. 2015; He et al. 2017; Wang 2018). Therefore, in the present study, reservoir pore evolution characteristics are researched based on reservoir

diagenesis and reservoir porosity with quantitative evaluation using casting thin sections, scanning electron microscopy (SEM), high-pressure mercury injection, cathodoluminescence, and other technical means. Reservoir rock types and their physical properties and pore structure are analyzed to better understand the reservoir characteristics and densification factors and provide a reference for reservoir evaluation and development in the study area.

Geological setting

The Ordos basin is a typical cratonic basin located in Central China with a stable basin structure and an east–west inclination angle of less than 1° (He 2003). On the plane, the basin can be divided into five first-level geological structural units: the Jinxi flexural fold belt in the east, the Tianhuan depression and fault-fold belt in the west, the Weibei uplift belt in the south, the Yimeng uplift belt in the north, and the Yishan slope in the center (Yao et al. 2015). Paleozoic, Mesozoic, and Cenozoic strata are developed in the basin, and the Mesozoic strata are the main terrestrial hydrocarbon generation beds and extra-low-permeability sandstone reservoirs (Zeng and Li 2009). The Ordos basin was a large inland lake when the Yanchang Formation of the upper Triassic was deposited, which developed a series of sedimentary strata from lake to lake retreat (Yao et al. 2015). The Yanchang Formation is divided into the Chang-10 to Chang-1 Members from bottom to top, of which the sedimentary period from Chang-10 to Chang-7 Member is the lacustrine basin expansion period, and the Chang-7 Member deposition period was the peak period for the development of the whole lacustrine basin, when the delta front subfacies developed with a thickness of 1000~1500 m (Yao et al. 2013; Lin et al. 2008).

The Xin'anbian area is located in the center of the Ordos basin and is structurally positioned in the west of the Yishan slope (Fig. 1) and has an area of around 5000 km². The Chang-7 Member in the research area is divided into three sub-members from bottom to top: the Chang-7₃, Chang-7₂, and Chang-7₁. The main part of Chang-7₃ is a semi-deep lacustrine deposit that contains a set of high-quality source rocks rich in organic matter. During the sedimentary period of the Chang-7₂, the water became shallower, and the sedimentary sand bodies of subaqueous distributary channel mainly developed in the delta front, which can be regarded as the main reservoir. Water inflow and retreat occurred repeatedly during the period spanning Chang 7₂ to Chang-7₁, and the hydrocarbon source rocks were interbedded with sandstone beds, forming favorable source-reservoir configuration relations and typical tight sandstone reservoirs (Fig. 2).

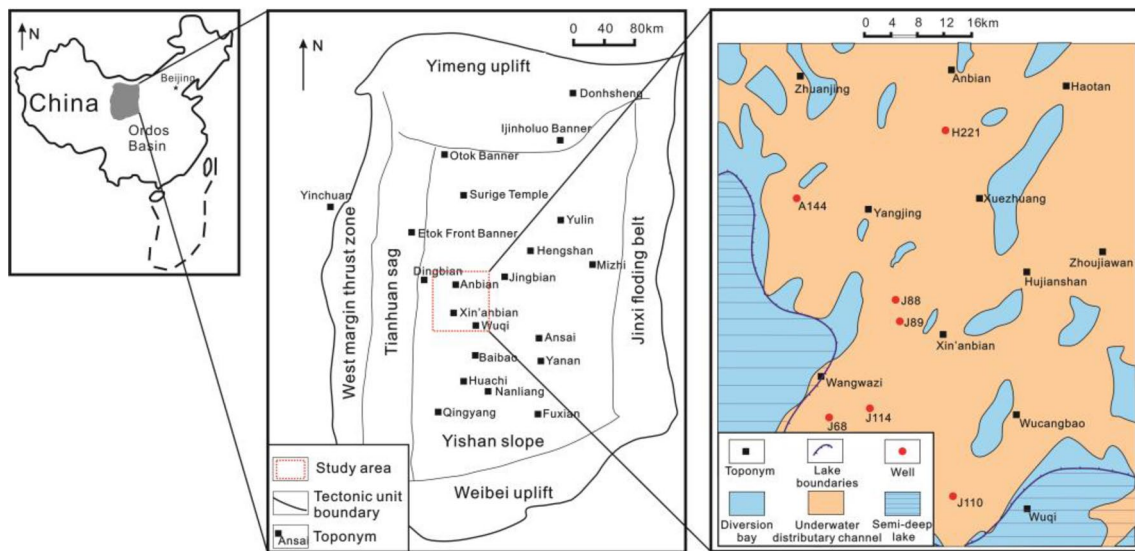


Fig. 1 Location map of the Xin'anbian Chang-7 Member in the Ordos basin (Yao et al. 2015; Hui et al. 2019)

Methodology

Main experimental methods

All experimental samples and data were from the Chang-7 Member of the Xin'anbian area of the Ordos basin. The porosity and permeability data for 2,156 samples from 14 wells were collected from the CNPC Changqing oil field branch. To effectively identify reservoir pore space and calcite cement, 32 cast thin sections in seven wells were prepared by blue epoxy resin filling and Alizarin Red S solution staining. The cast section was observed at the Key Laboratory of Deep Oil and Gas of China University of Petroleum in east China with the ZEISS Axio imager D1m. After the preparation and gold plating of 11 compact sandstone samples by SEM, an E-T secondary electronic detector was used to observe the microscopic pores and autogenous minerals in the reservoir under the working voltage of 10.00 kV and working distance of about 29.6 mm using a coxemem-30 scanning electron microscope. The mineral composition analysis was carried out by combining X-ray energy spectra. The SEM observation and energy spectrum analysis were completed in the Key Laboratory of Deep Oil and Gas of China University of Petroleum in east China. Standard column samples with a diameter of 2.5 cm were prepared for 14 compact sandstone samples, and high-pressure mercury injection experiments were carried out using the PoreMaster 60 high-pressure mercury injection instrument in the laboratory of reservoir characteristics and percolation mechanism of China University of Geosciences. This allowed the pore size distribution and capillary pressure curves of the reservoir to be obtained.

Methods of reservoir quantitative evaluation

(1) Quantitative evaluation of diagenesis

Compaction, cementation, and dissolution are the most important diagenesis. The three parameters of the apparent compaction rate, apparent cementation rate, and apparent dissolution rate were introduced to quantitatively describe the diagenesis degree of tight sandstone reservoirs in the study area (Chu et al. 2013).

The apparent compaction ratio could be used to represent the degree of compaction of the initial pores in the reservoir (Zhang et al. 1997), and the calculation formula was as follows:

$$\alpha = (\Phi_1 - \Phi_{ce} - \Phi_{ori}) / \Phi_1 \times 100\%, \quad (1)$$

where α is the compaction rate, Φ_1 is the initial porosity, Φ_{ce} is the integral number of cementing objects, and Φ_{ori} is the intergranular porosity.

In general, $\alpha < 30\%$ indicated weak compaction strength, $30\% < \alpha < 70\%$ medium compaction, and $\alpha > 70\%$ strong compaction.

The apparent cementation rate could be used to quantitatively express the effect of cementation on the sandstone reservoir. The formula was as follows:

$$\beta = \Phi_{ce} / \Phi_1 \times 100\%, \quad (2)$$

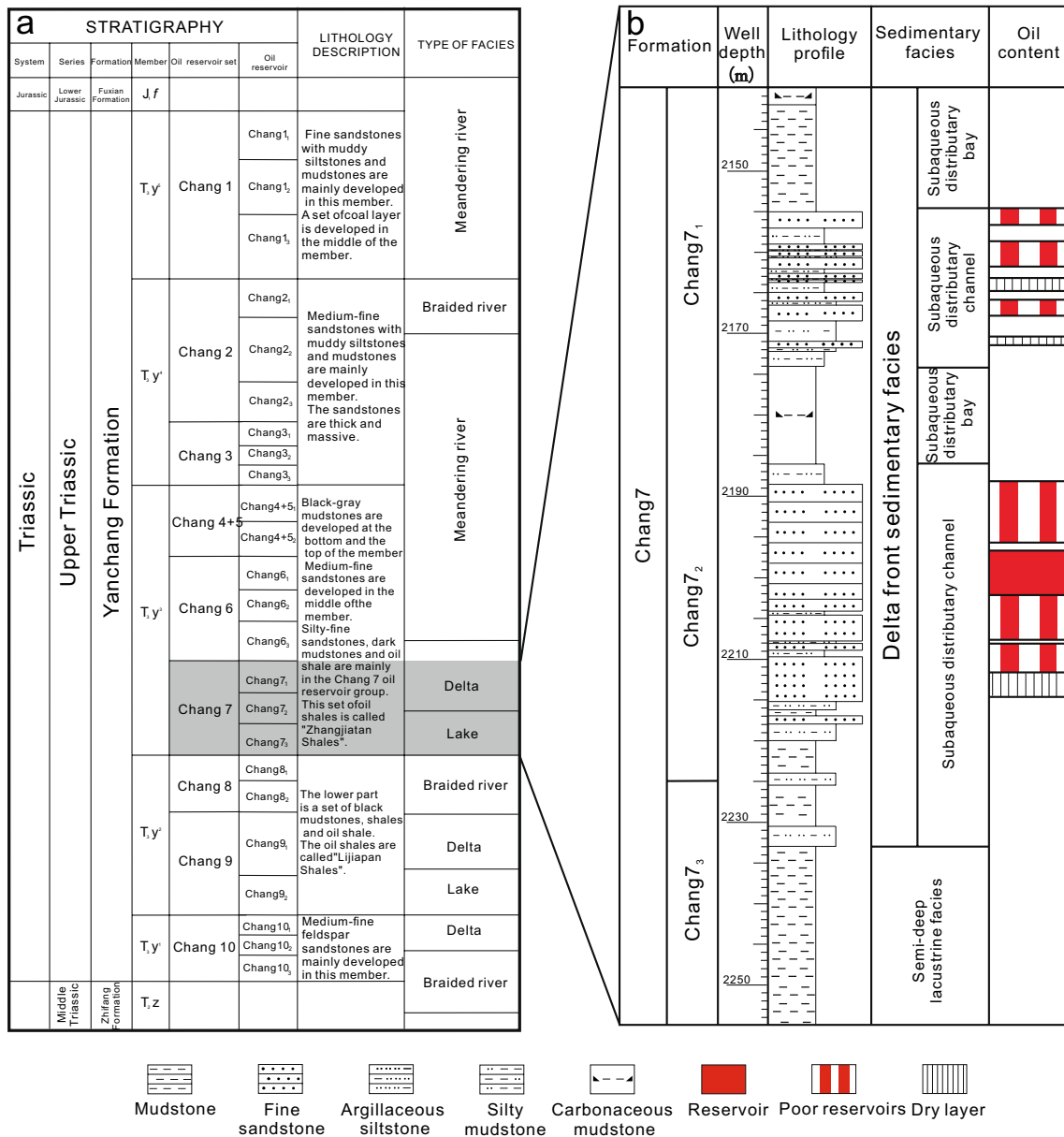


Fig. 2 Column diagram of the Triassic strata in the Ordos basin (a) (revised according to Xu et al. 2017) and comprehensive diagram of the strata in the Chang-7 Member of the Xin'anbian area (b)

where β is the apparent cementation rate, Φ_{ce} is the initial porosity, and Φ_1 is the integral number of cementing objects.

$\beta < 30\%$ indicated weak cementation, $30\% < \beta < 70\%$ medium cementation, and $\beta > 70\%$ strong cementation.

The apparent dissolution rate could quantitatively describe the dissolution degree of the reservoir, and the calculation formula was as follows:

$$\gamma = \Phi_{diss} / \Phi_{por} \times 100\%, \tag{3}$$

where γ is the apparent dissolution rate, Φ_{diss} is the dissolution rate of pore faces, and Φ_{por} is the total face rate.

$\gamma < 25\%$ represented weak corrosion, $\gamma < 25\%$ medium dissolution, and $\gamma > 60\%$ strong corrosion (Cheng et al. 2010).

(2) Methods of calculating porosity evolution

Methods for determining the original porosity.

The initial porosity of reservoir samples was calculated according to the formula used to calculate the initial

porosity of equal-sized spherical particles proposed by Beard and Weyl (1973):

$$\Phi_1 = 20.91 + 22.90/S_0, \quad (4)$$

where Φ_1 is the initial porosity and S_0 is the trask sorting coefficient [$S_0 = (Q_1/Q_3)^{1/2}$]; Q_1 is the first quartile, which was equivalent to the particle size at 25%; and Q_3 was the third quartile, which corresponds to the particle size at 75%.

To quantitatively characterize the effect of compaction and cementation on reservoir densification, the following parameters were quoted:

$$\Phi_2 = \Phi_{ce} + [(\Phi_{ori} + \Phi_{ced})/\Phi_{por}] \times \Phi_n \quad (5)$$

$$\Phi_3 = \Phi_n \times \Phi_{ori}/\Phi_{por} \quad (6)$$

$$L_1 = \Phi_1 - \Phi_2 \quad (7)$$

$$L_2 = \Phi_2 - \Phi_3 \quad (8)$$

$$F_1 = L_1/\Phi_1 \text{ (Beard and Weyl 1973)} \quad (9)$$

$$F_2 = L_2/\Phi_1 \text{ (Cheng et al. 2010)}, \quad (10)$$

where Φ_1 represented the initial porosity, Φ_2 the compaction residual porosity, Φ_3 the cementing residual porosity, L_1 the compaction loss porosity, L_2 the cementation loss porosity, F_1 the compaction porosity loss rate, F_2 the cementing porosity loss rate, Φ_{ce} the total cement content, Φ_n the present porosity, Φ_{ori} the intergranular pore face rate, Φ_{ced} the pore dissolution rate of the cement, and Φ_{por} the total face rate.

Results

Petrological characteristics

Chang-7 Member reservoir rocks in the Xin'anbian area are mostly comprised of coarse siltstone and less so of fine siltstone and fine sandstone, and the rock types are mainly lithic feldspathic sandstone and feldspathic detritus sandstone (Fig. 3). The quartz content in lithic feldspathic sandstone is 17~37% (average content is 30.3%), the feldspar content is 15~30% (average content is 23.1%), the lithic content is 4~19% (average content is 14%), and the mica content is 0~10% (average content is 4%). Feldspathic detritus sandstone has a quartz content of 20~34% (average content of 27.2%), a feldspar content of 11~29% (average content of

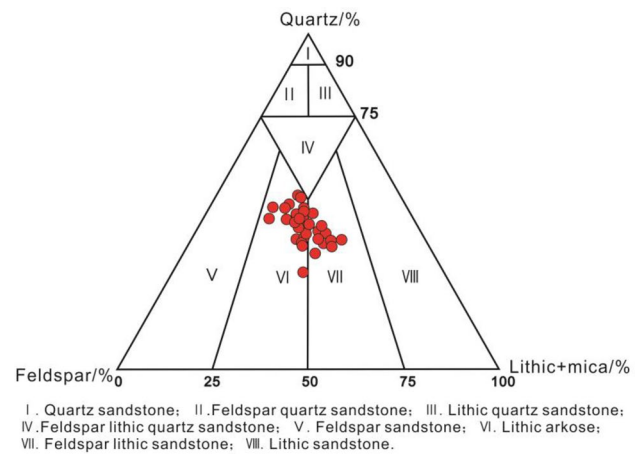


Fig. 3 Identification of rock types in the Chang-7 Member reservoir of the Xin'anbian area

19%), a lithic content of 7~29% (average content of 16.2%), and a mica content of 3~20% (average content of 9.9%).

The types of interstitium in the study area mainly included carbonate cement such as calcite, clay cement such as kaolinite, and a small amount of siliceous and ferric cement (Fig. 4). The total content of interstitium was between 18 and 52%. There were some differences in the types and contents of the interstitial materials in the different rock types, among which the calcareous content of lithic feldspathic sandstone was around 17.8% and argillaceous content around 10%, while the calcareous content of feldspathic detritus sandstone was around 13.3% and argillaceous around 13.9%.

Physical characteristics of the reservoir

The statistical results of the porosity and permeability of 1673 reservoir samples (Figs. 5 and 6) indicated that the porosity of the tight sandstone in the Chang-7 Member in the Xin'anbian area ranged from 0 to 16%. The average of porosity was 7.13%, most of which was in the range of 4~10%, accounting for 76% of the total. The permeability ranged from 0 to 12 mD, and the average of permeability was 0.102 mD, most of which was between 0.01 and 1 mD, accounting for 93% of the total. Zhao Chenglin (Zhao et al. 1998) divided the classification criteria of pore permeability in the Ordos basin in 1998. He identified the reservoirs with a porosity of 15~10% and a permeability of $50 \times 10^{-3} \sim 10 \times 10^{-3}$ mD as low porosity and low-permeability reservoirs and the reservoirs with a porosity of 10~5% and permeability of $10 \times 10^{-3} \sim 1 \times 10^{-3}$ mD as extra-low porosity and extra-low-permeability reservoirs. Furthermore, he identified reservoirs with a porosity of <5% and permeability of $1 \times 10^{-3} \sim 0.1 \times 10^{-3}$ mD as extra-low porosity and extra-low-permeability

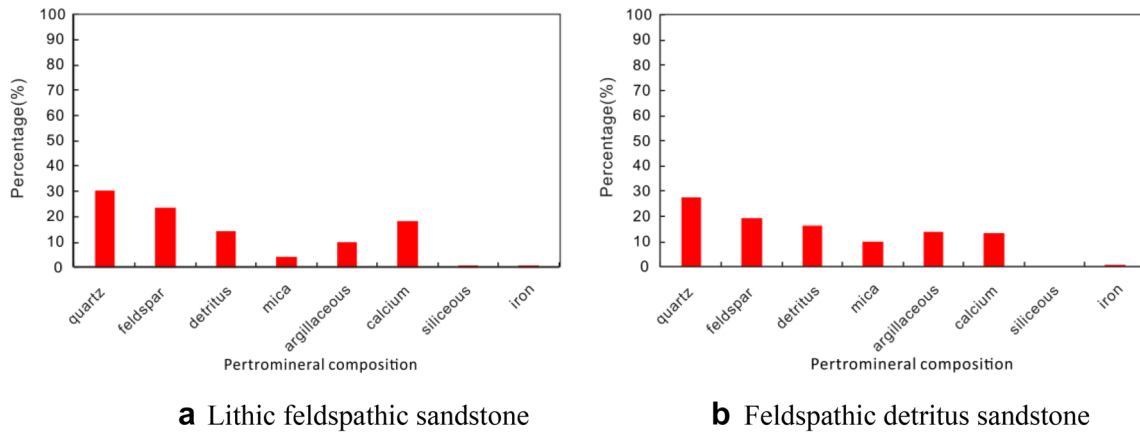


Fig. 4 Rock composition comparison in the Chang-7 Member reservoir of the Xin'anbian area

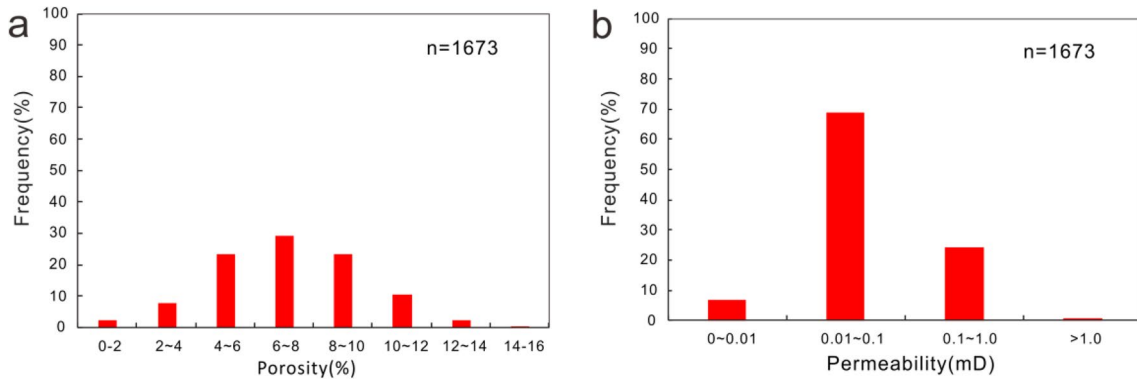
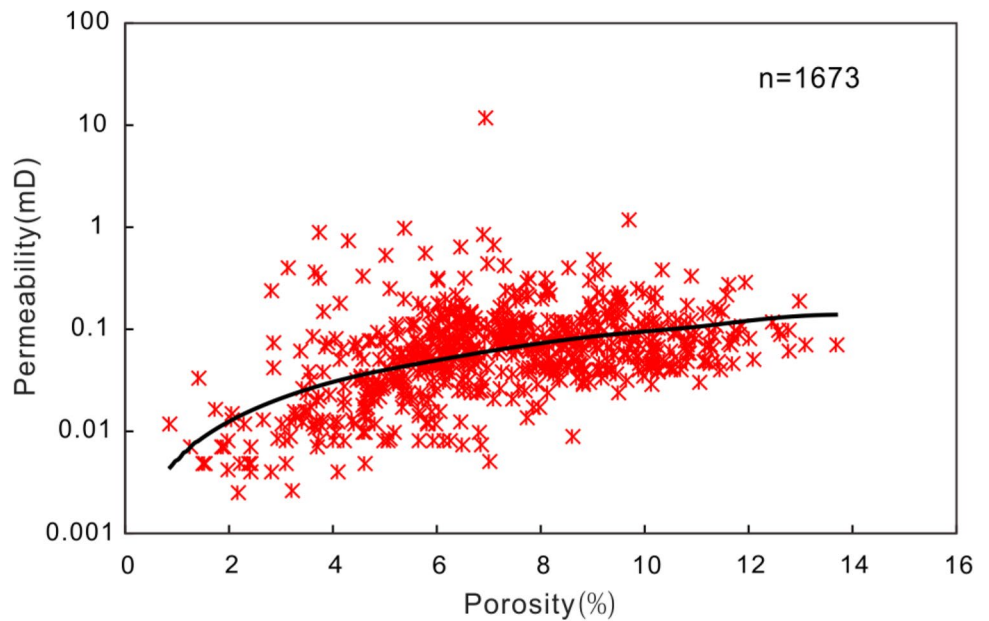


Fig. 5 Frequency distribution of the porosity (a) and permeability (b) in the Chang-7 Member reservoir of the Xin'anbian

Fig. 6 Crossplot of the porosity and permeability in the Chang-7 Member reservoir of the Xin'anbian area



reservoirs. In 2009, Hu Wenrui et al. (Hu 2009; Zhao et al. 2012) improved the above permeability classification standard, identifying reservoirs with a permeability of $10 \times 10^{-3} \sim 1.0 \times 10^{-3}$ mD as general low-permeability reservoirs, those with a permeability of $1.0 \times 10^{-3} \sim 0.5 \times 10^{-3}$ mD as extra-low-permeability reservoirs, and those with a permeability below 0.5×10^{-3} mD as extra-low-permeability reservoirs. According to the above classification scheme, the Chang-7 Member tight sandstone reservoirs in the study area can be divided into low porosity and extra-low-permeability reservoirs and extra-low porosity and extra-low-permeability reservoirs. The porosity and permeability of the Chang-7 Member reservoirs showed a positive correlation according to the crossplot of reservoir porosity and permeability, but the data distribution was relatively discrete, reflecting the complex formation of the reservoir and indicating that it was highly heterogeneous.

Reservoir space

The types of space in the Chang-7 Member reservoir in Xin'anbian area could be divided into primary pores, secondary pores, and microfractures according to their genesis. The primary pores were mainly residual intergranular pores (Fig. 7a), with good connectivity between the pores and flakier throat. The secondary pores were mainly intracrystalline dissolved pores of feldspar grains (Fig. 7b, c, d, e, f, g), followed by intercrystalline pores of clay minerals (Fig. 7i). The dissolution pores in feldspar grains were mostly distributed along the cleavage of feldspar (Fig. 7b, c, e, g). Some feldspar edges had dissolved to form dissolution pores (Fig. 7d, f), and certain clay minerals, such as kaolinite and intergranular pores of kaolinite, had developed in the reservoirs in the study area (Fig. 7i). There were also some microfractures in the quartz grains in the reservoir (Fig. 7h) that were relatively straight.

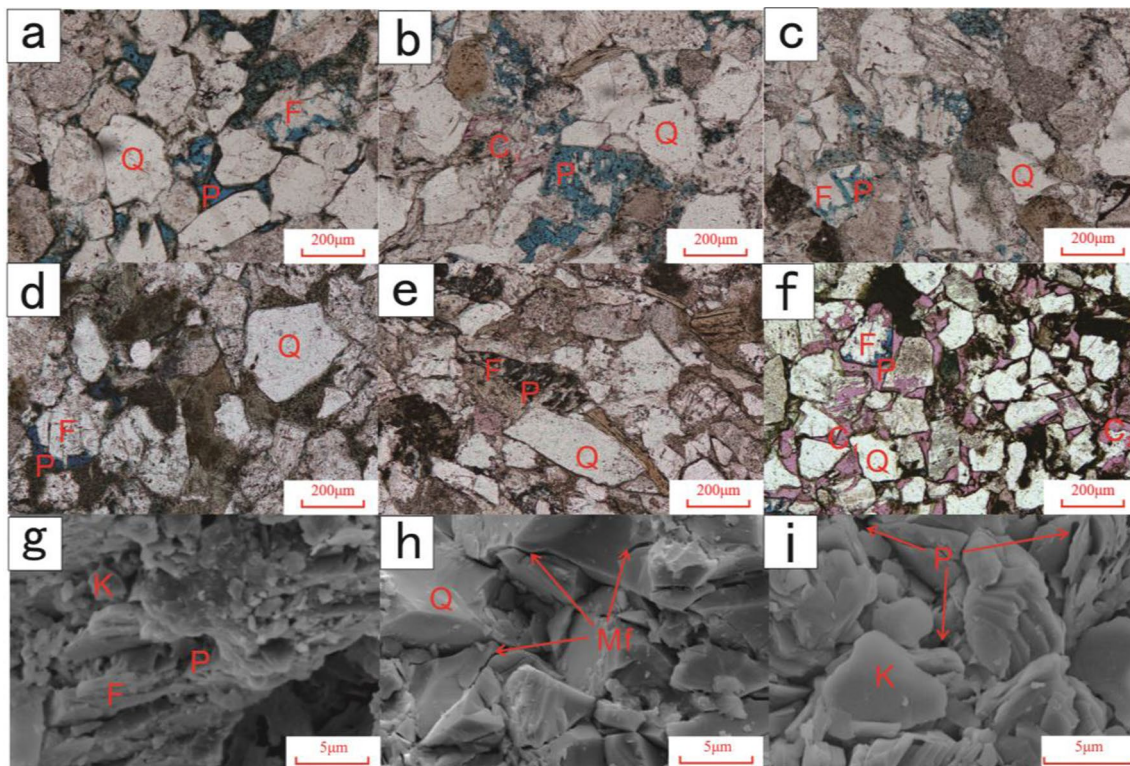


Fig. 7 Reservoir space type in the Chang-7 Member of the Xin'anbian area. **a** Residual intergranular pores (P) and a few dissolved pores developed between quartz (Q) and feldspar (F) grains, J89, 2241.15 m; **b** Cementation of calcite (C_1) between quartz (Q) grains, development of feldspar intergranular dissolution pore (P), intergranular dissolution pore (J89, 2,251.5 m); **c** An intrapolytic pore (P) developed along the cleavage seam of feldspar (F), H221, 2179.48 m; **d** Some feldspar particles were dissolved at the edges to form intergranular dissolution pores (P), H221, 2203.6 m; **e** Feldspar was dissolved along the cleavage fractures, with a few feldspar dis-

solution pores (P), H221, 2199.4 m; **f** The contact between the quartz (Q) and feldspar (F) particles was point contact, and there was calcite (C_1) cementation between grains. Most feldspar dissolution pores were filled with calcite (C_2), and there were a small number of residual dissolution pores in grains (P), J110, 2183.2 m; **g** Feldspar was dissolved along cleavage fractures, with small dissolution pores (P) and a small amount of kaolinite (K) on the surface, J110, 2169.6 m. **h** Development of internal microcracks (Mf) in quartz grains, H221, 2199.4 m. **i** Intercrystalline pores (P) of page-shaped kaolinite (K) developed, J88, 2274.68 m

The statistical results of the pore radius of the Chang-7 Member reservoir in different reservoir spaces (Fig. 8) showed that the residual intergranular pores in the reservoir in the research area had a large pore radius of 10~60 μm , although the number of pores was small. The dissolution pores of feldspar were the most common pores in the research area and had a wide range of pore sizes (0.05~60 μm), among which > 1 μm feldspar dissolution pores had a large diameter but few in number. The particle sizes of feldspar dissolution pores in the research area were mainly 0.1~1 μm , the number of pores accounted for about 70% of all the pores, and the peak of the pore size distribution was 0.3~0.5 μm , which was the main type of pore in the reservoir. The width of the microfractures ranged from 0.05 to 1 μm . The presence of microfractures helped to enhance the connectivity between the pores in the reservoir. The pore size of clay intergranular pores was small and most was less than 0.5 μm . The peak of the pore size was around 0.1~0.3 μm . The comparison showed that the number of residual intergranular pores and the volume of clay intergranular pores and microfractures in Chang-7 Member reservoir were small, and the feldspar dissolved pores were relatively developed, which is the main reservoir space type of the Chang-7 Member reservoir.

Main diagenesis of reservoir

(1) Compaction

Compaction has an important effect on primary pores, and the strength of compaction mainly depends on the depth of burial and the mineral composition of rocks (Chu et al.

2013). Plastic cuttings (such as mica, argillaceous cuttings) gradually deform, elongate, and fill the pores, thereby reducing reservoir porosity (Fig. 11a, b, c) under the influence of compaction. Generally, the compression compaction of a reservoir increases and the porosity and permeability decrease with the increase of reservoir burial depth.

As shown in Fig. 9, the porosity decreased from 13 to 8%, and the permeability decreased from 3 to 0.1 mD when the buried depth increased from 2240 to 2400 m. That is, porosity and permeability decrease with depth. However, it contradicts the above phenomenon that the porosity increased from 8 to 13%, and the permeability increased from 0.1 to 7 mD when the buried depth of reservoir was within the range of 2150~2240 m. According to the statistics for quartz, feldspar, and rock chip particles in the reservoir, the percentage of brittle particles such as quartz, feldspar, and igneous rock chips in this range was the highest, accounting for about 57~67% of the total volume of reservoir rocks, while the content of the brittle particles in the reservoirs outside this range was lower than 55% (Fig. 10).

(2) Cementation

Some primary and secondary pores in the reservoir were filled by rock cement, which reduced the physical properties of the reservoir (Yang 2013). The cementation of the Chang-7 Member reservoir in the Xin'anbian area was relatively developed. The cementation types were mainly calcite calcareous cementation, clay mineral argillaceous cementation, and a small amount of silica secondary enlargement and other siliceous cementation (Fig. 15d) and iron cementation (Fig. 11c, i). There were two stages of calcite cementation in

Fig. 8 Frequency distribution of the pore radius of different pores in the Chang-7 Member of the Xin'anbian area

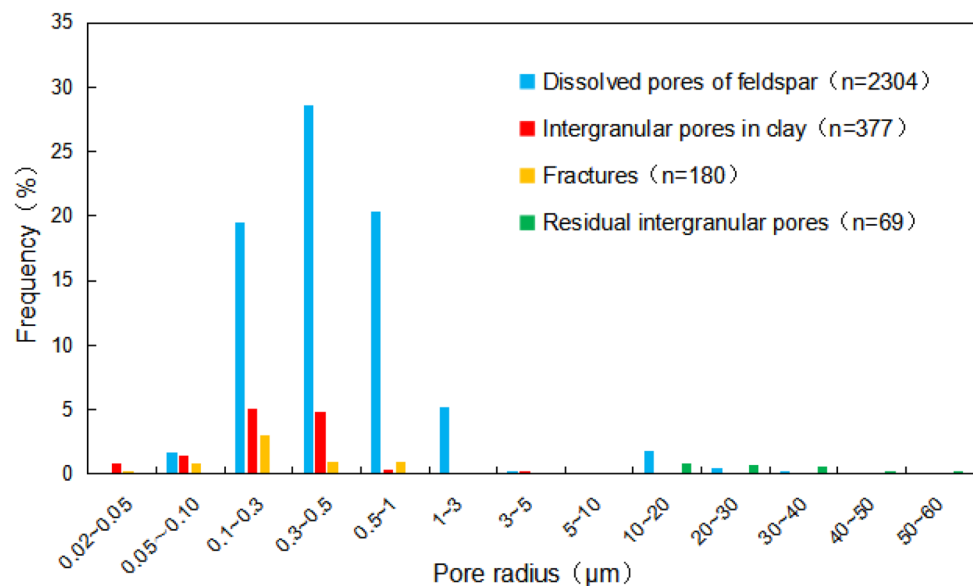


Fig. 9 Change in porosity and permeability with depth in the Chang-7 Member reservoir of the Xin'anbian area

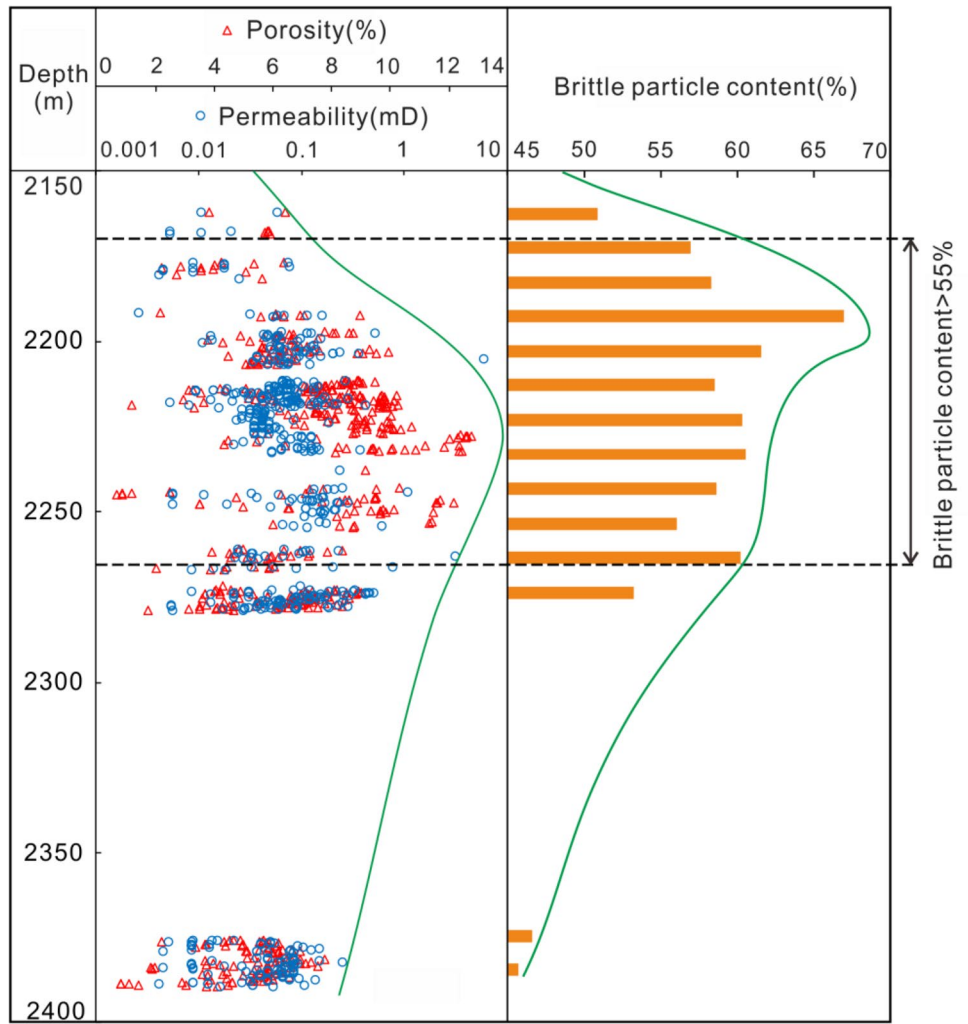
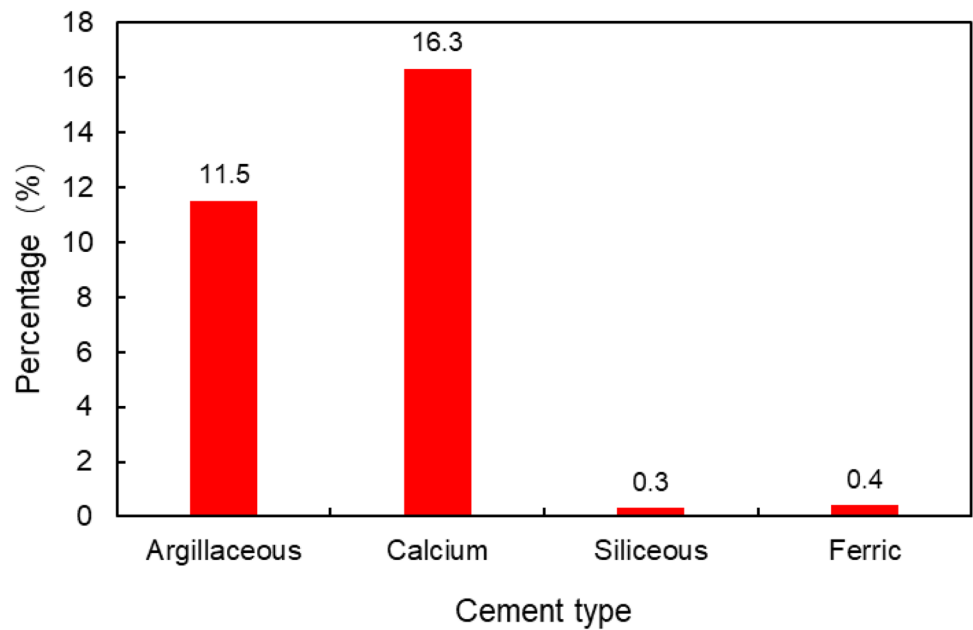


Fig. 10 Cementing type and distribution in the Chang-7 Member reservoir of the Xin'anbian area



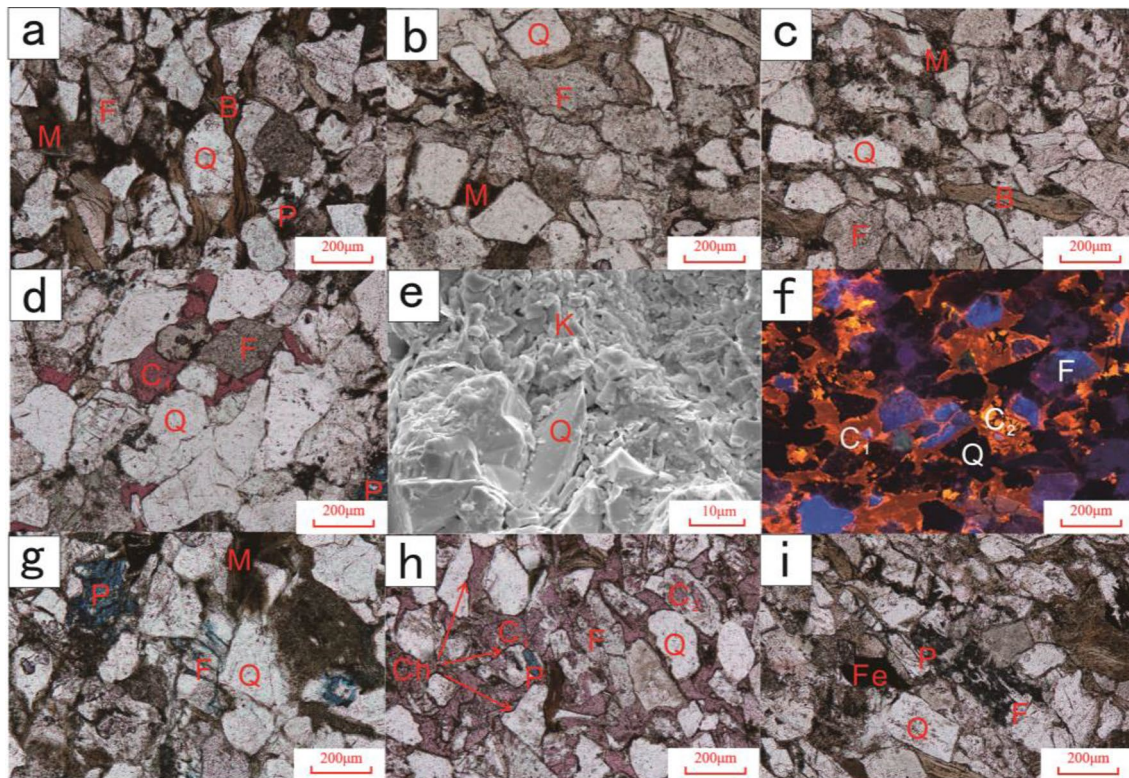


Fig. 11 Typical diagenesis in the Chang-7 Member reservoir of the Xin'anbian area. **a** Plastic particles such as biotite (B) are deformed by compression compaction, intergranular particles are filled with argillaceous (M), and a small number of ingranular dissolved pores (P) are developed, J68, 2232 m; **b** Press-dissolution between feldspars and argillaceous (M) fillings between grains, H221, 2199.4 m; **c** Grains of quartz (Q) and feldspar (F) were filled with a small amount of argillaceous (M), and biotite (M) was compressed and deformed, H221, 2199.4 m; **d** Calcite was cemented in intergranular (C_1), quartz (Q) was increased, intergranular microchimerism was tight, and some feldspar was dissolved into the dissolution pores (P), J89, 2251.5 m; **e** kaolinite (K) filled around quartz (Q) grains with unde-

veloped intergranular pores, H221, 2199.4 m; **f** Calcite was cemented between particles (C_1), and some calcite filled the feldspar dissolution holes (C_2), J88, 2274.68 m; **g** Feldspar granules (F) were dissolved along the cleavage crack internally and developed intracellular dissolution pores (P) with argillaceous (M) cementation, H221, 2203.6 m; **h** Calcite was cemented between particles (C_1), and some feldspar (F) was dissolved and filled with calcite (C_2), containing a small number of ingranular dissolution pores (P). There was a layer of chlorite film (Ch) on the surface of the particles (J68, 2220.24 m). **i** A small amount of iron (Fe) cement between grains, internal dissolution of feldspar, H221, 2199.4 m

the study area that formed in the early transition from montmorillonite to illite and in the late dissolution of feldspar (Xi et al. 2018). Argillaceous cement was widely distributed. The argillaceous cement was mainly kaolinite (Fig. 11e), and there was a small amount of illite and chlorite cement.

(3) Dissolution

Feldspar corrosion was common in the Chang-7 Member reservoir in the Xin'anbian area, and feldspar was mostly dissolved in grains or dissolved along cleavage, forming ingrain pores. The solution hole formed by feldspar dissolution was usually filled with cementitious material in areas where cementitious action was strong (Fig. 11h).

Discussion

Effects of major diagenesis on physical properties of reservoir

Previous studies have proved that diagenesis can be regarded as the main controlling factor of reservoir densification (Li et al. 2006; Zhong et al. 2012; Chen et al. 2013; Wang et al. 2014; Jin et al. 2017). Diagenesis is divided into constructive diagenesis and destructive diagenesis. Mechanical compaction, quartz secondary enlargement, carbonate cementation, clay mineral filling and so on will damage the pores of the reservoir and reduce the physical properties of the reservoir (Zhang 2008; Yang et al.

2012; Li et al. 2013), while the dissolution of carbonate and feldspar, the intergranular pores of kaolinite and the rim of chlorite play a constructive role in the development of reservoir pores (Li et al. 2004; Zhang 2008). Thus, different diagenesis will have different effects on reservoir physical properties.

The diagenesis of Chang-7 Member tight sandstone reservoir mainly included compaction, dissolution, and cementation (Fig. 11). Compaction and cementation destroy reservoir's physical properties, while dissolution improves reservoir's physical properties.

(1) Compaction

Compaction can reduce reservoir's physical properties, and its effect is influenced by reservoir depth and rock composition. According to Fig. 12, the brittle particle content in the Chang-7 Member reservoir was positively correlated with reservoir porosity, indicating that the higher brittle mineral particle content in reservoir led to relatively strong compaction resistance, which is conducive to the preservation of primary pores and thus to relatively high porosity and permeability. Combined with the distribution of particle content of different properties in the study area, the areas with a higher content of argillaceous particles in the study area had poor anti-compaction ability and strong compaction, while areas with a higher content of brittle particles had a strong anti-compaction ability and weak compaction effect.

(2) Cementation

The study area was dominated by calcareous cementitious and argillaceous cementitious materials, which filled the intergranular pores and made the reservoir's physical properties poor. Clay mineral cementation usually destroys the primary pores by filling them, though sometimes a chlorite

film is formed on the surface of the rock particles to prevent secondary expansion of quartz and protect the primary pores (Fig. 11h).

(3) Dissolution

Dissolution, especially of feldspar minerals, is an important way of improving the physical properties of tight reservoirs. The dissolution of feldspar and other minerals can effectively improve the physical properties of a reservoir. However, due to the strong cementation in some areas, cementation can fill partial dissolution holes, reduce reservoir capacity, and worsen a reservoir's physical properties.

Quantitative evaluation of the main diagenesis of the reservoir

The effect of diagenesis on the physical properties of a reservoir can be quantitatively characterized by the apparent compaction rate, cementation rate, and dissolution rate (Zhang et al. 1997; Cheng et al. 2010; Chu et al. 2013). By quantitatively calculating and comparing the apparent compaction rate, cementation rate, and dissolution rate of a single well with formulas 1, 2, and 3 (Fig. 13), it was determined that the apparent compaction rate of the Chang-7 Member reservoir in the Xin'anbian area was mostly between 10 and 47%, among which wells H221 and J89 were higher, while wells A144 and J110 were lower, showing weak to medium compaction. According to the isopach maps of sandstone in the study area (Fig. 14), the sand body in the study area had an axis of symmetry from east to west in the north and thinned on both sides. Wells H221, J89, J68, J88, and J114 were distributed along the axis and the sand body > 20 m, with strong compaction under pressure and tight arrangement among particles. However, wells A144 and J110 had relatively thin sand bodies and weak compression compaction.

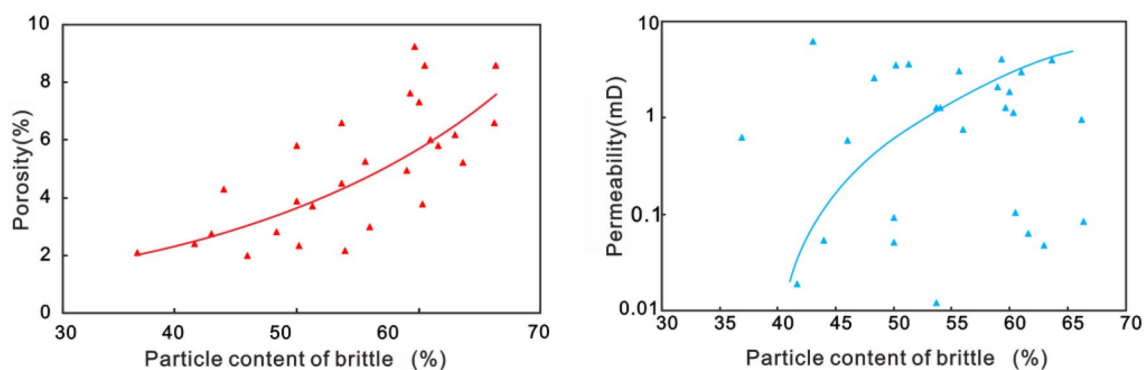
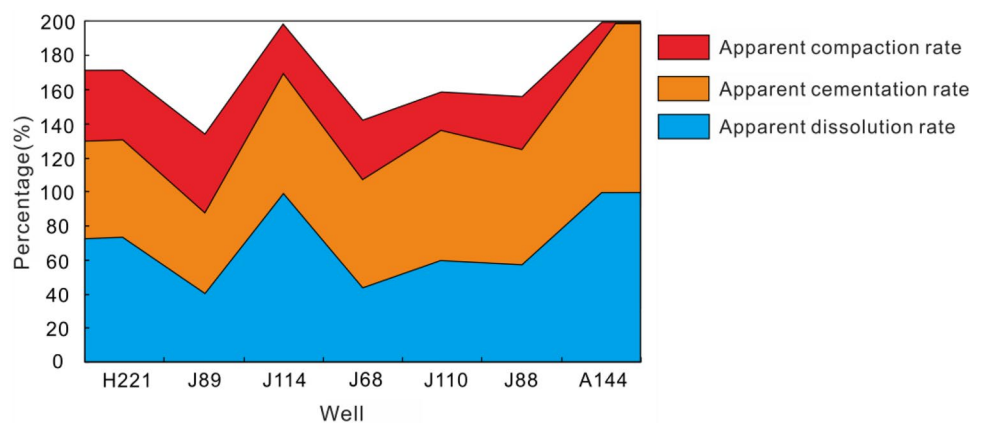


Fig. 12 Effect of brittle particle content on porosity and permeability in the Chang-7 Member reservoir of the Xin'anbian area

Fig. 13 Diagenesis parameter distribution and reservoir classification map in the Chang-7 Member reservoir of the Xin'anbian area



The apparent cementation rate of the Chang-7 Member reservoir was between 40 and 90%, among which wells A144 and J110 were relatively high, while wells H221 and J89 were relatively low, showing medium and strong cementation. As can be seen from Fig. 14, the areas with a high apparent cementation rate in the study area tended to have a low apparent cementation rate. This was because a large number of intergranular pores were preserved in the areas with weak compaction under compression, which provided space for filling with cement in the later stages. For this reason, the apparent cementation rate was high. However, in areas with strong compression compaction, the formation was closely arranged among grains, with a large number of intergranular pores, and late cementing did not easily fill, so the cementation rate was relatively low. The dissolution degree of the Chang-7 Member reservoir was quite different. Wells J114, A144, and others had a relatively large apparent dissolution rate and strong dissolution effect, while wells J89, J68, and others had a relatively weak dissolution effect.

In conclusion, the study area as a whole by weak-medium compaction, medium-strong cementation and different degrees of dissolution. The strength of compaction and cementation is controlled by the thickness of reservoir sand body to a certain extent. In the area with larger sand body thickness, the compaction is stronger but the cementation is weaker; otherwise, the compaction is weaker but the cementation is stronger.

From the above analysis, it can be concluded that the Chang-7 Member reservoir in the research area had a significant impact on compaction and cementation, which is the main reason for the densification of tight sandstone reservoirs. This study found certain differences to the research results of Chu et al. (2013), Wang and Qiu (2018). To further compare the impact strength of compaction and cementation on reservoirs, the degree of porosity loss (Beard and Weyl 1973; Cheng et al. 2010) caused by compaction and cementation was compared (Fig. 15). The cementation of the reservoir in the study area increased with the decrease

of compaction, where cementation reduced porosity by 15~30% and 25% on average, while compaction reduced porosity by 10~20% and 13% on average. In other words, cementation reduced porosity more than compaction.

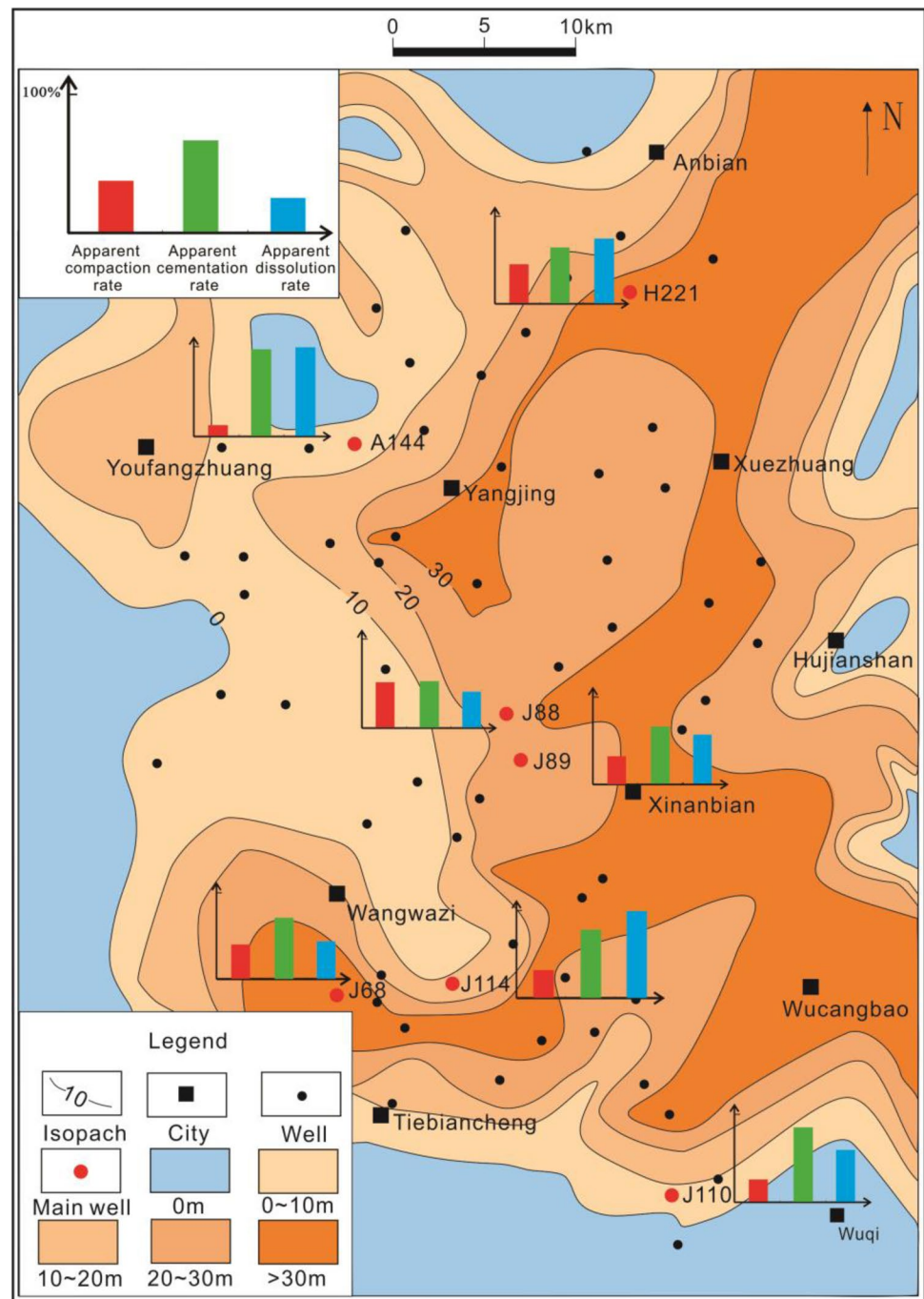
According to the analysis chart of compaction and cementation pore reduction strength of 23 samples (Fig. 16), the compaction and cementation strength of the Chang-7 Member reservoir in the research area varied greatly, and the diagenesis strength of different samples was relatively dispersed. For example, porosity loss rate of cementation was distributed between 25~95%. The porosity loss rate of cementation was higher than the rate of compaction in 18 samples, indicating that cementation played a major role in damaging the physical properties of the reservoir.

Reservoir porosity evolution

Due to the complex diagenetic evolution process of tight sandstone in the study area, when conducting a comprehensive analysis of the porosity evolution characteristics in the study area, it was assumed that each diagenetic phenomenon was relatively independent. First, according to formula (4), the initial porosity of the reservoir in the study area was around 39%. The pore evolution of the reservoirs in the study area was mainly influenced by compaction, cementation, and dissolution. According to the development characteristics of the main diagenesis of the reservoirs and previous diagenesis research results, the pore evolution process of the Chang-7 Member tight sandstone reservoirs in the Xin'anbian area could be divided into four stages (Fig. 17).

The first stage spanned the Triassic to the Early Jurassic period, during which time the main compression compaction lost around 13% porosity, and the remaining compaction porosity was 26%. The second stage was from the Middle Jurassic to the Late Jurassic period, when cementation began and the physical properties of the reservoir further deteriorated. In this period, the reservoir porosity decreased by nearly 21%, and the remaining cementation porosity was 5%. The

Fig. 14 Quantitative distribution of sandstone thickness and diagenesis in the Chang-7 Member reservoir of the Xin'anbian area



third stage started from the Early Cretaceous, when a large number of hydrocarbons were generated from the source rocks. Hydrocarbon filling caused the fluid to become acidic (Wang 2018), which promoted the dissolution of feldspar and rock debris and the secondary increase of quartz, as well as forming secondary pores. The mesodiagenetic stage A followed, where the porosity increased by about 6–11% until the late Early Cretaceous period. From the late Early Cretaceous to the early Late Cretaceous period, as hydrocarbon filling gradually ended, the reservoir slowly returned to an alkaline

environment, secondary calcareous cementation occurred, and the porosity decreased by 4%. Until the Late Cretaceous period, the stratum was uplifted, diagenesis was weakened, and the pores did not change a great deal, reaching the present porosity.

Fig. 15 Frequency distribution of porosity loss due to compaction and cementation in the Chang-7 Member reservoir of the Xin'anbian area

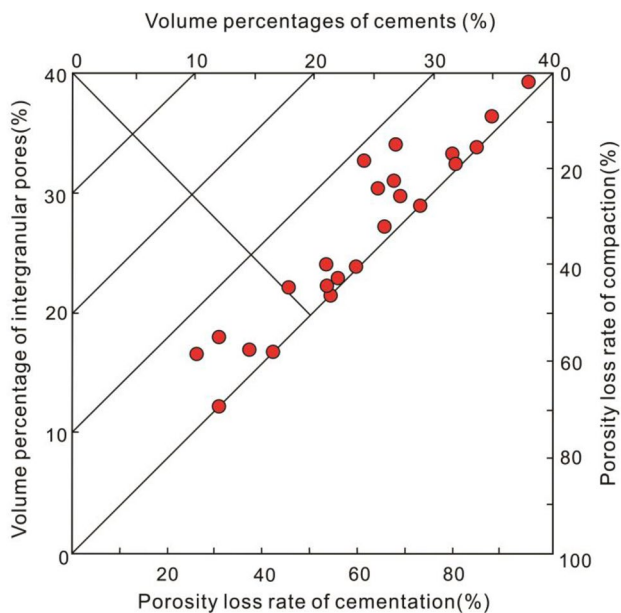
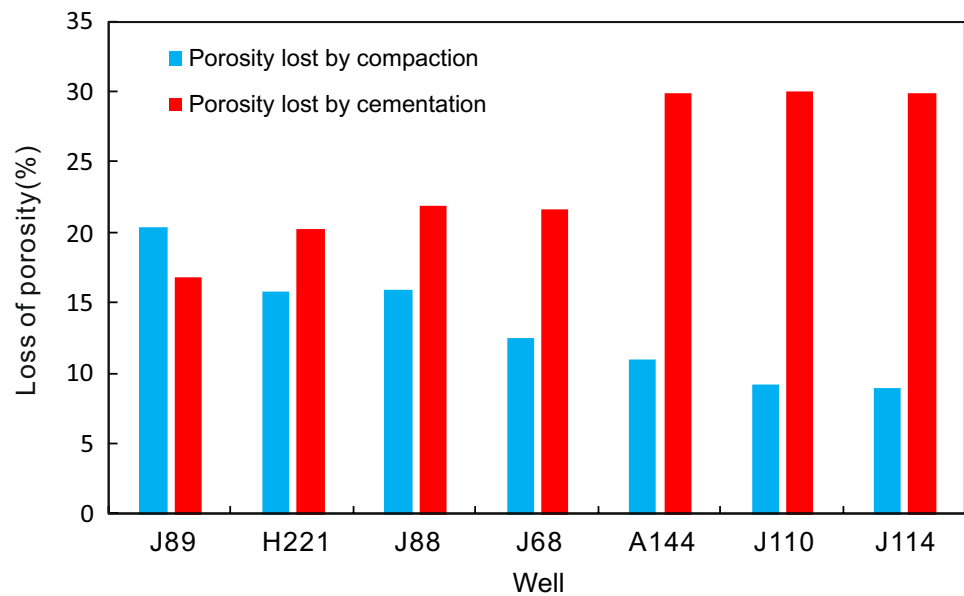


Fig. 16 Pore reduction strength analysis diagram of compaction and cementation of different types of tight sandstone reservoirs in the Chang-7 Member of the Xin'anbian area [the chart refers to Lundegard (1992), Wang and Qiu (2018)]

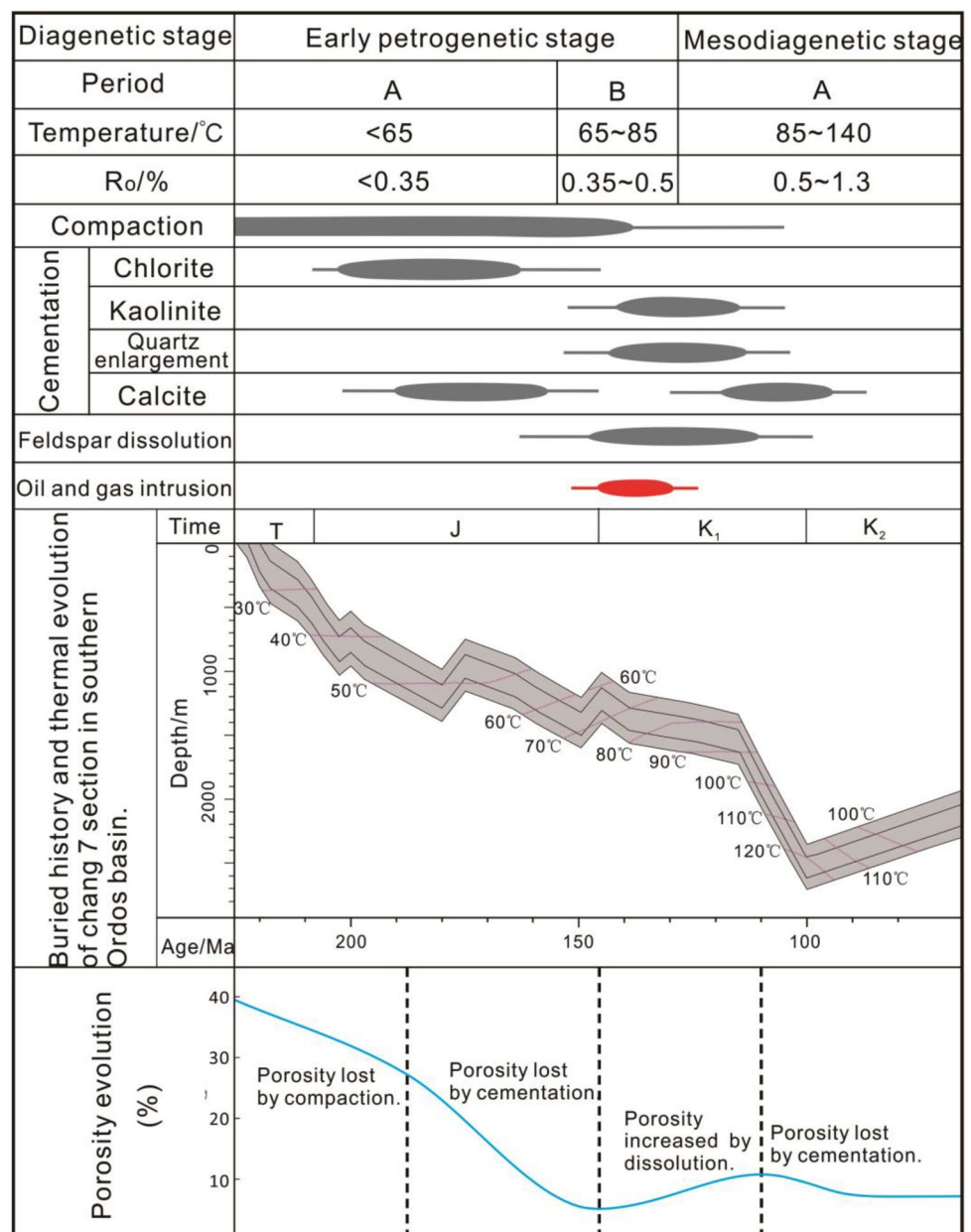
Conclusion

(1) Chang-7 Member reservoir rock types in the Xin'anbian area are mainly lithic feldspathic sandstone and feldspathic detritus sandstone. The reservoirs can be classified as low porosity and low permeability and extra-low porosity and extra-low permeability. The porosity and

permeability of the reservoirs are mainly controlled by compaction, cementation, and dissolution, among which compaction and cementation reduce the porosity and permeability of the reservoirs, and corrosion improves their physical properties.

- (2) The apparent compaction rate of the Chang-7 Member reservoir in the study area was mainly between 10~47%, while the apparent cementation rate was between 40~90%, and the apparent dissolution rate was >40%. The Chang-7 Member reservoir mainly experienced weak-medium compaction, medium-strong cementation, and different degrees of dissolution. The average porosity loss of cementation was around 25%, while the average porosity loss of compaction was about 13%. In other words, cementation played a major role in the destruction of the physical properties of the reservoirs.
- (3) Comprehensive analysis showed that the porosity evolution of the Chang-7 Member in the study area could be divided into four stages: (1) the porosity in study area was reduced to 26%, mainly due to compression compaction from the Triassic to the Early Jurassic period; (2) the cementation seriously damaged the reservoir from the Middle Jurassic to Late Jurassic, and the porosity decreased to 5%; (3) in the Early Cretaceous period, the porosity increased to 11% due to dissolution; and (4) the porosity was reduced to 7%, which was mainly due to cementation from the late Early Cretaceous to early Late Cretaceous period.

Fig. 17 Diagenesis and pore evolution model in the Chang-7 Member tight sandstone reservoirs of the Xin'anbian area [buried history according to Yang chao (Yang et al. 2018)]



Acknowledgements This study was financially supported by the National Natural Science Foundation of China (41702142), the Fundamental Research Funds for the Central Universities and the Development Fund of Key Laboratory of Deep Oil & Gas (20CX02110A).

References

- Beard DC, Weyl PK (1973) Influence of texture on porosity and permeability of unconsolidated sand. *Am Assoc Petrol Geol Bull* 57:349–369
- Chen ZB, Zhu YS, Chen XJ et al (2013) Sedimentation and diagenesis of Chang 8² reservoir in the Yanchang Formation in Jiyuan region, Ordos Basin. *Oil Gas Geol* 34(5):685–693
- Cheng QG, Zhang L, Zheng HN, Gong FH (2010) Classification and significance of diagenetic reservoir facies based on quantitative characterization of diagenesis—a case study of ultra-low permeability reservoir of yanchang 6 oil formation in wangyao xinghe hou city, ordos basin. *J Pet Natl Gas* 32(05):60–65
- Chu MJ, Guo ZQ, Qi YL, Cheng DX (2013) Quantitative diagenesis and diagenetic facies analysis of yanchang 8 reservoir in Ordos basin. *Natl Gas Geosci* 24(03):477–484
- Fan MM (2016) Study on tight reservoir characteristics of Triassic Yanchang in Ordos basin. Northwest University, Evanston
- He ZX (2003) Evolution and oil and gas in ordos basin. Petroleum Industry Press, Beijing
- He CK, Cheng LB, Chen XF, Sun TX, Li C, Zhao GX (2017) Identification of effective tight oil reservoirs and selection of deserts in xinanbian oilfield, ordos basin. *Pet Exp Geol* 39(06):812–818

- Hu WR (2009) Introduction to low-permeability oil and gas fields. Petroleum Industry Press, Beijing, p 246
- Hui HN, Peng P, Zhao LL et al (2019) Controls of organic and inorganic compositions on pore structure of lacustrine shales of Chang 7 member from Triassic Yanchang Formation in the Ordos Basin, China. *Mar Petrol Geol* 100:270–284
- Jin J, Kang X, Hu WX et al (2017) Diagenesis and its influence on coarse clastic reservoirs in the Baikouquan Formation of western slope of the Mahu Depression, Junggar Basin. *Oil Gas Geol* 38(2):323–333
- Li QD (2016) Study on tight oil reservoir characteristics of An83-Chang7 in Xin'anbian oilfield. Northwestern University, Evanston
- Li HJ, Wu TR, Ma ZJ et al (2004) Research on the basic characteristics and control factors of high-quality reservoir in Sulige gas field. *Natl Gas Ind* 24(8):12–13
- Li H, Liu YQ, Liu LY (2006) Diagenesis of Chang 81 reservoir with low permeability in Xifeng oilfield, Ordos Basin. *Oil Gas Geol* 27(2):209–217
- Li YL, Jia AL, He DB (2013) Control factors on the formation of effective reservoirs in tight sands: examples from Guang'an and Sulige gasfields. *Acta Pet Sin* 34(1):71–82
- Liang DG, Ran LH, Dai DS, He ZX, Ou YJ, Liao S, He WY (2011) Reunderstanding of the exploration potential of large area of unconventional oil in the Jurassic system in the north central Sichuan basin. *Acta Petroleologica Sin* 32(01):8–17
- Lin HB, Hou HC, Chen HD, Hong HY (2008) Characteristics and evolution of sedimentary system in yanchang formation of upper Triassic in ordos basin. *J Chengdu Univ Technol* 35(06):674–680
- Lundegard PD (1992) Sandstone porosity loss: a “big picture” view of the importance of compaction. *J Sediment Res* 62(2):250–260
- Meng WC, Meng XZ, Chen LJ, Leng DF, Wang CX, Wang XP, Yang DX, Pan ZK, Huang ZX (2018) Evaluation of tight oil resources in chang 6, chang 7 and chang 8 sections of Yanchang in the southern Ordos basin. *Energy Environ Protect* 40(11):144–151
- Sun ZD, Jia CZ, Li XF et al (2011) Unconventional oil and gas exploration and development. Petroleum Industry Press, Beijing, pp 1–150
- Wang YN (2018) Coupling relationship between diagenetic evolution and accumulation formation in tight reservoir of xinbian oilfield in Ordos basin. China University Of Geosciences, Beijing
- Wang Z, Qiu JL (2018) Effects of compaction and cementing on Chang 8 reservoir in Ordos. *J Southwest Pet Univ* 40(06):56–68
- Wang F, Chen R, Tian JC et al (2014) Diagenesis and diagenetic facies of the Chang 4+5 tight sandstone reservoirs in Longdong area, Ordos Basin. *Oil Gas Geol* 35(2):199–206
- Wu PT, Yao ZG, Wu WT, An XS, Ning B (2018) Study on the formation time of tight sandstone oil reservoirs in southeast Chang 7 of Ordos basin. *Liaoning Chem Ind* 47(10):1068–1070
- Xi KL, Cao YC, Liu KY, Wu ST, Yuan GH, Zhu RK, Kashif M, Zhao YW (2018) Diagenesis of tight sandstone reservoirs in the Upper Triassic Yanchang Formation, southwestern Ordos Basin, China. *Mar Pet Geol*. <https://doi.org/10.1016/j.marpetgeo.2018.10.031>
- Xu ZJ, Liu LF, Wang TG, Wu KJ, Gao XY, Dou WC, Xiao F, Zhang NN, Song XP, Ji HT (2017) Application of fluid inclusions to the charging process of the lacustrine tight oil reservoir in the Triassic Yanchang Formation in the Ordos Basin. *China J Petrol Sci Eng* 149:40–55
- Yang J (2013) Characteristics of tight sandstone reservoirs of chang 4+5 formation in yan'an area of ordos basin. *Litholog Reserv* 25(6):28–32
- Yang RC, Wang XP, Fan AP et al (2012) Diagenesis of sandstone and genesis of compact reservoirs in the East II part of Sulige gas field, Ordos Basin. *Acta Sediment Sin* 30(1):111–119
- Yang C, He YH, Ma FX, Lei YH, Chen YG (2018) Division of organic fluid activity stages in the Triassic yanchang formation in the southern ordos basin. *Natl Gas Geosci* 29(05):655–664
- Yao JL, Deng XQ, Zhao YD, Han TY, Chu MJ, Pang JL (2013) Tight oil characteristics of yanchang formation in ordos basin. *Oil Explor Dev* 40(02):150–158
- Yao YT, Li SX, Zhao YD, Chen SJ, Lu JG (2015) Characteristics and control factors of tight oil in xinbian region of Ordos basin. *Acta Sediment Sin* 33(03):625–632
- You Y, Niu XB, Feng SB, Wang F, Wang CY, Li WC (2014) Study on micro pore characteristics of tight oil reservoirs in yanchang 7 of Ordos basin. *J China Univ Pet* 38(06):18–23
- Zeng LB, Li XY (2009) Fractures in sandstone reservoirs with ultra-low permeability: a case study of the Upper Triassic Yanchang Formation in the Ordos Basin. *China AAPG Bull* 93(4):461–477
- Zhang SN (2008) Tight sandstone gas reservoirs: Their origin and discussion. *Oil Gas Geol* 29(1):1–10
- Zhang YW, Xiong QH, Wang ZZ (1997) Continental reservoir description. Petroleum industry press, Beijing, pp 98–117
- Zhang H, Chen G, Zhu YS, Dang YC, Chen J, Wang HL, Si Y, Bai C, Li X (2017) Quantitative characterization of micro pore structure in tight oil reservoirs: a case study of Chang 7 reservoir in Xin'anbian oilfield. *Ordos Basin Pet Exp Geol* 39(01):112–119
- Zhao CL, Hu AM, Chen BY et al (1998) SY/T 6285–1997, oil and gas reservoir evaluation method (oil and gas industry standard of the People's Republic of China). Petroleum industry press, Beijing
- Zhao JZ, Bai YB, Cao Q, Er C (2012) Quasi-continuous low-permeability and tight sandstone reservoir formation model in Ordos basin. *Oil Gas Geol* 33(06):811–827
- Zhong DK, Zhou LJ, Sun HT et al (2012) Influences of petrologic features on diagenesis and pore development: an example from the Triassic Yanchang Formation in Longdong area, Ordos Basin. *Oil Gas Geol* 33(6):890–899
- Zou CN, Zhang GG, Tao SZ, Hu SY, Li XD (2010) Geological characteristics, major discoveries and unconventional petroleum geology in the global oil and gas exploration field. *Oil Explor Dev* 37(02):129–145
- Zou CN, Yang Z, Tao SZ, Li W, Wu ST, Hou LH, Zhu RK, Yuan XJ, Wang L, Gao XH, Jia JH, Guo QL, Bai B (2012) Oil and gas accumulation by nano-oil and gas with source and reservoir symbionism. *Pet Explor Dev* 39(01):13–26
- Zou CN, Tao SZ, Hou LH et al (2013a) Unconventional oil and gas geology. Geology press, Beijing
- Zou CN, Zhang GS, Yang Z, Tao SZ, Hou LH, Zhu RK, Yuan XJ, Ran QQ, Li DH, Wang ZP (2013b) Concept, characteristics, potential and technology of unconventional oil and gas—on unconventional oil and gas geology. *Petr Explor Dev* 40(04):385–399

Publisher's Note Springer Nature remains neutral with regard to jurisdictional claims in published maps and institutional affiliations.